Fundamentals of Acoustic Beamforming

Leandro de Santana
Department Thermal Fluid Engineering
University of Twente
P.O. Box 217
Enschede, 7500 AE
The Netherlands

leandro.desantana@utwente.nl

ABSTRACT

The acoustic beamforming is an instrumental tool applied to the localization and quantification of acoustic sources. This technique has been proven in a large range of academic and industrial applications along the years showing to be very robust, efficient and accurate. This lecture note discusses the fundamentals of delay-and-sum and conventional beamforming and the deconvolution techniques DAMAS, DAMAS2, CLEAN-PSF and CLEAN-SC. Additionally, it is shown some application examples in simulated and experimental aeroacoustic sound sources, followed by a discussion about some strengths and limitations of each algorithm.

Contents

1.0   INTRODUCTION

Noise is a modern societal problem that, among other consequences, hinders the installation of large wind turbines close to residential areas and limits the number of take-offs and landings in large airports. In recent years, the academia and industry joined efforts to propose noise reduction solutions which significantly contributed to the keep the noise issue under certain level of control.

The beamforming technique is one of the most successful noise localization and quantification approaches able to support designers and engineers to rank and quantify individual noise sources. This technique is very robust allowing to distinguish sources even in challenging situations when the source intensity is many decibels below the background noise level. This capacity allows designers and engineers to more precisely evaluate (innovative) noise reduction solutions.

From an historical perspective, the beamforming technique is predeceased by elliptic acoustic mirrors [1–4] (see Fig. 1). This approach assumes sound waves propagating as acoustic rays. Accordingly to the description presented in Fig. 1, assuming that the noise source is located in the acoustic far-field (in relation to the measurement position), it is possible to focus the acoustic mirror on any point where the noise source is expected to be (acoustic focal point F_2). Therefore, the microphone placed in the acoustic focal point F_1 will measure the source strictly located in the point F_2. This signal can be Fourier-transformed allowing to quantify the sound source intensity at specific frequency bands.
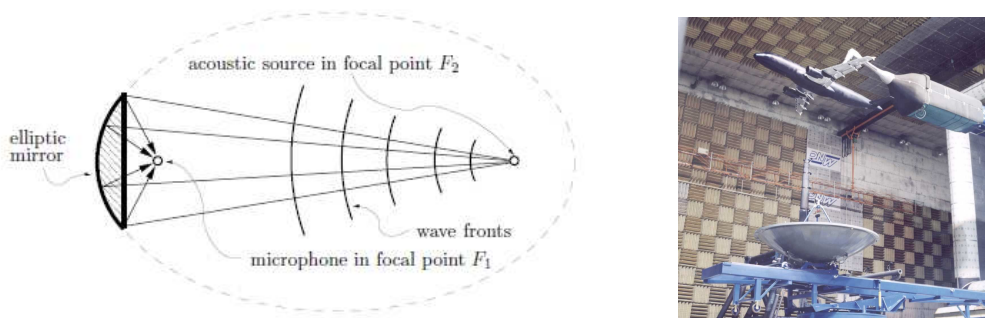

Figure 1: Schematic representation of the working principle of an acoustic mirror (left) and set-up with an acoustic mirror in DNW-LLF open jet facility (right). Source: left [4]; right [5].

The elliptic mirror performs "spatial filtering" allowing to efficiently distinguish closely located noise sources practically removing the background noise influence. This technique was largely applied until the early 90's in the localization of acoustic sources in academic and industrial wind tunnel environments such as the DNW-LLF facility (Fig. 1 right). However, the elliptic mirror represents to be an expensive technique to be applied in large industrial wind tunnel facilities. The large cost is related with the low-productivity of this technique since, for each measurement point, the mirror has to be mechanically moved with help of an accurate traverse system. After that, data should be sampled for some seconds or minutes (depending the required precision), turning the process long and tedious.

After the middle 90's, advances in digital computers, development of fast data acquisition system, large capacity and fast data storage, turned the microphone array techniques highly attractive to perform acoustic noise source localization and quantification. Nowadays, the technological development of hardware and software allows experimental researchers to efficiently build (or purchase) very robust microphone arrays equipped with more than a hundred of microphones. This large technological leap made possible performing very refined noise source localization in full size wind turbines, scaled aircrafts placed in industrial wind tunnels and real

size aircrafts flying over microphone arrays placed on the ground (see Fig. 2).
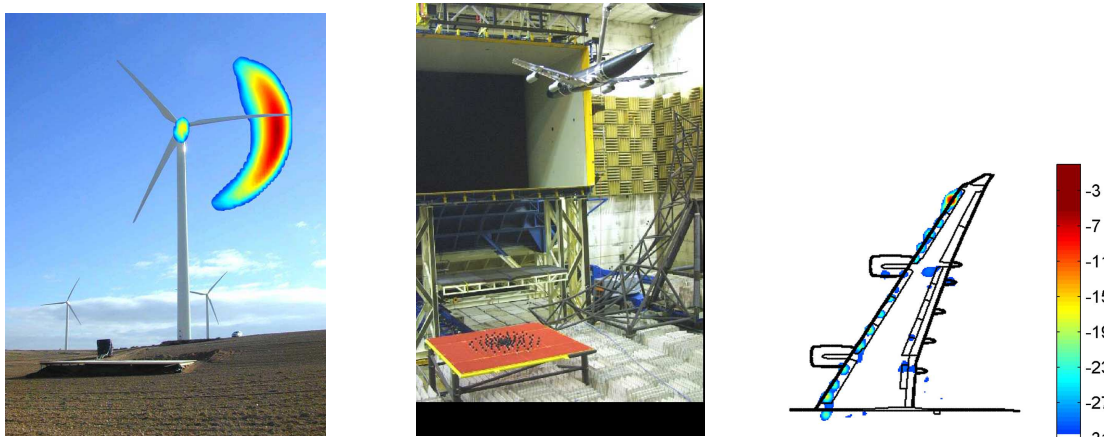

Figure 2: Beamforming applied to wind turbine noise source localization (left); center and right: wind tunnel airframe noise testing. Source: left [6]; center [7]; right [4].

The microphone array is the most complex instrumentation required in the application of the beamforming technique. Figure 3 shows an example of an airfoil noise measurement performed in the University of Twente Aeroacoustic Wind Tunnel. In Fig. 3 (left) the flow comes from the left to the right direction. Since this wind tunnel has an open test section, the microphone array can be placed outside the flow reducing significantly the influence of the pressure fluctuation induced by the flow into the signal measured by the microphones. In this case the CAE Systems Bionic M-112 microphone array equipped with 112 digital MEMS microphones is used. This array uses digital microphones and a FPGA digital data acquisition system. With the fast development of the smart phones, nowadays we have increasingly high-quality miniaturized digital microphones. Due to the massive production of those applied to the telecommunication, they are nowadays available in the market for purchase for a couple of Euros. Furthermore, digital data loggers have currently a more affordable price per channel than analog data acquisition systems. Furthermore, digital protocols allows perform data multi-plexing which significantly reduces the number of physical channels required for data acquisition. This recent technological innovation allows to reduce the cost per channel of a microphone array by a factor of up to one hundred. Turning, therefore, the beamforming microphone array technique application in product development affordable to small and medium size companies.

2.0 FUNDAMENTALS

2.1 Microphone data acquisition

The beamforming technique applied to noise source localization and quantification requires the frequency do-main interpretation of the pressure signal acquired by each microphone of the array. The acoustic pressure is a physical continuous signal that has to be digitally interpreted in the beamforming processing. The beamform-ing technique considers an array of M spatially distributed microphones and the typical analog data acquisition chain of each sensor is schematically represented in Fig. 4.

In this schematic representation, the acoustic wave excites the microphone membrane producing an small AC voltage that is amplified in the microphone preamplifier in order to reduce the influence of the electronic noise produced by the cables and connections that conduct the information to the amplifier. The amplified
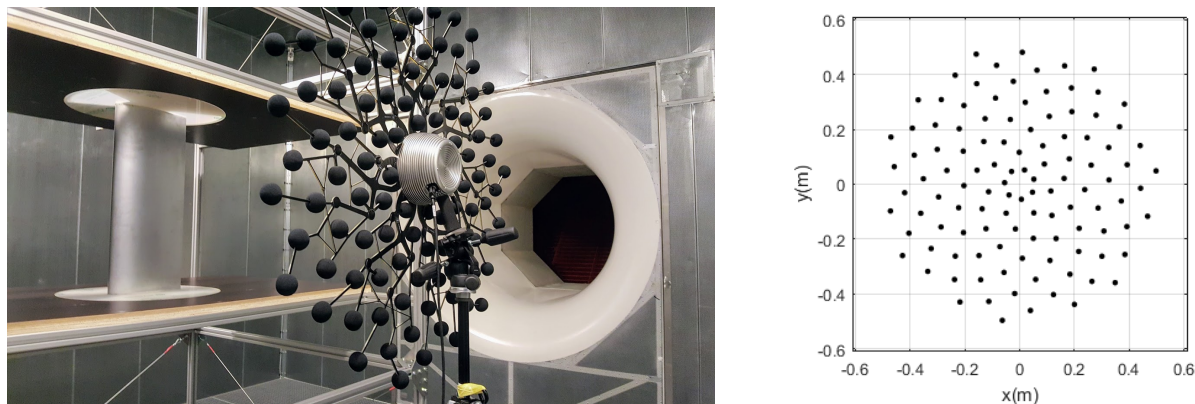
Figure 3: Left: Example of application of a beamforming microphone array in the localization and quantification of acoustic sources in a wind tunnel airfoil noise measurement. Test performed in the *University of Twente Aeroacoustic Wind Tunnel*. Right: example of the microphone distribution in the array. The sensors placement "seems" to be random, however they are optimized such to improve the array performance. The left figure is published under authorization of LM Wind Power.
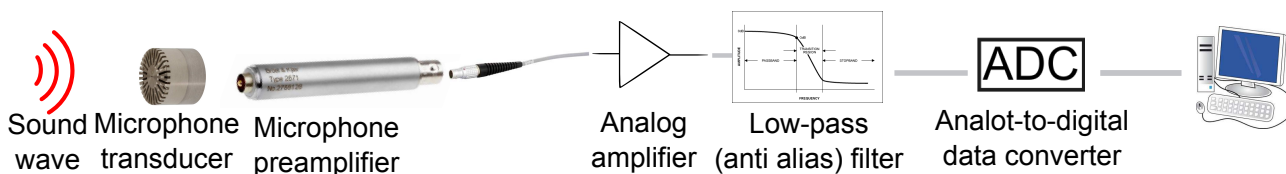

Sound wave | Microphone transducer | Microphone preamplifier | Analog amplifier | Low-pass (anti alias) filter | Analot-to-digital data converter

Figure 4: Schematic representation of the microphone data acquisition system.

signal is then low-pass filtered to avoid the alias effect in the analog-to-digital conversion. The reader is invited to check the references [8, 9] for further details about the analog-to-digital conversion process and details about critical problems, e.g. aliasing, in the digital data sampling. After this step, the continuous microphone signal $p(t)$ is stored in the computer memory as a discrete set of data $p(n\Delta t)$ sampled at constant time steps $\Delta t = 1/f_s$, where f_s is the sampling frequency and n is an integer number.

The acquired data has to be Fourier-transformed in order to be represented in the frequency domain and allow the application of more complex post-processing beamforming techniques. The Fast-Fourier-Transform algorithm is used for this propose. Considering a block with K samples the discrete Fourier-Transform relates the time domain pressure $p(n\Delta t)$ with the complex valued (therefore representing the phase and amplitude information) frequency domain pressure as:

$$p(f) = \frac{2}{K} \sum_{n=1}^{K} p(t) e^{-2\pi i \, f \, n \, \Delta t}. \tag{1}$$

The Fast-Fourier-Transform algorithm requires the size of the Fourier-transformed data block K be a power of 2. Furthermore, the pressure $p(f)$ is available at discrete frequencies:

$$0 \leq n \frac{f_s}{K} \leq \frac{f_s}{2}, \tag{2}$$

where n is an integer number, the discrete Fourier-transform results that the frequency domain data is represented now discrete frequencies in steps of an integer number multiplied by f_s/K and the upper limit is $f_s/2$

which is the Nyquist frequency which indicates that the digital data conversion process cannot represent data with frequency higher than half of the sampling frequency. This happen because (roughly speaking) it is required a minimum of two points to represent a sine or a cosine wave. Therefore, the energy content in the signal relative to waves with more than half of the sampling frequency "folds back" being interpreted by the digital data converter as low-frequency waves contaminating, therefore, the acoustic spectrum. This justifies the mandatory presence of a analog low-pass filter in the data acquisition chain, represented in Fig. 4 which is able to remove from the signal the energy of the waves with frequency above $f_s/2$.

The beamforming technique requires the estimation of the Cross-Spetral-Matrix (CSM) – which will be discussed in detail later. The spectral estimator of the microphone cross-power pair is defined as:

$$C_{mn} = \mathrm{E}(p_m(f)p_n^*(f)) \,, \tag{3}$$

where m and n represents the microphone number.

Considering that the stochastic process is ergodic, i.e. given enough time it can be represented in terms of statical parameters, the ensemble average of the previous equation can be replaced by the time average, therefore the cross-power spectrum can be estimated as:

$$C_{mn} = \frac{1}{N} \sum_{n=1}^{N} p_m(f)p_n^*(f) \,, \tag{4}$$

however, in real-world, every measured signal is contaminated by noise, e.g. electronic interference, turbulent flow reaching the microphone inducing the so-called pseudo noise, etc. Therefore the cross-power estimator can be written considering the noise influence as:

$$C_{mn} = \mathrm{E}\left[(p_m(f) + \xi_m(f))(p_n(f) + \xi_n(f))^*\right] \,, \tag{5}$$

where $\xi(f)$ corresponds to the noise here considered as a random phenomena. Considering that the noise component of the signal has zero mean and variance σ. Assuming that the noise is statistically independent from the (acoustic) signal intended to be measured, the cross-correlation between noise signal measured by two different channels should be equal to zero. Therefore, the cross-power estimator is represented as:

$$C_{mn} = \mathrm{E}(p_m(f)(p_n(f))^*) + \sigma^2\mathbf{I} \,, \tag{6}$$

where the term $\sigma^2\mathbf{I}$ is the statistical variance of the noise. Due to the statistically independence of the noise measured by two different channels, if the sampling time is long enough, off-diagonal CSM elements have uncorrelated noise and therefore they will be equal to zero. While the diagonal elements (auto-power) will be equal to the statistical variance of the noise. Therefore, an important result to keep in mind, in the application of the beamforming technique, is that the noise only influences the diagonal elements of the cross-spectral matrix. In practical situations where the microphone is subjected to flow, e.g. closed test section wind tunnel measurements, the pseudo-noise induced by the turbulent flow interacting with the microphone surface can significantly contaminate the CSM diagonal elements. This consequently requires use of advanced techniques such as diagonal removal in order to minimize this effect [9].

The cross-spectral matrix C_{mn} represents therefore an statistical estimation of the measured signal. Among the methods to estatistically estimate the CSM, the Welch method [10] is the most broadly used. For those who program in Matlab, this algorithm is already programmed in the function *pwelch* (for auto-spectra) and *cpsd* (for cross-power spectrum estimation). For completeness, the description of the Welch algorithm is presented:

1. The original data segment is split up into (typically 50%) overlapping segments of 2^n samples each (integer n);

2. The segments are then windowed (rectangular, triangular, Hanning, Hamming, etc);

3. For each segment, compute the periodogram by computing the discrete Fourier transform;

4. For the chosen microphone pair, multiply the periodogram;

5. Average the periodogram (this reduces the variance);

6. The end result is an array of cross-power measurements versus the frequency "bin".

2.2 Acoustic waves

For completeness, a brief discussion about points necessary to understand the beamforming technique are presented. The reader is recommend to read books such as Pierce [11] for more complete and didactic explanations about acoustics and Dowling [12] for aeroacoustics.

The acoustic sources localization by the beamforming technique is only possible due to the fact that acoustic waves have finite propagation speed that only depends of the medium (air, water, etc...) and temperature. In air at 27°, the sound propagates at 347 m/s. This property results that the sound wave produced by a given source will present different phase depending on the propagation distance. Therefore, each microphone in the array will "perceive" a different phase and, by knowing the sensors location, the source position consequently is found.

The source modeling in acoustic beamforming of fundamental importance. In acoustics and aeroacoustics, it is common practice to represent complex noise sources as a combination of monopole, dipole and quadrupole elementary sources. For extra literature please check: [11–13]). Most of the standard beamforming techniques also assume that the distance between source and observer is large enough and the microphone array diameter is sufficiently small to guarantee that the source directivity pattern does not play an important role and, therefore, complex acoustic sources can be well approximated by a distribution of monopole sources. Alternatively, when the microphone array is placed in the near-field of the acoustic source we have the Near-field Acoustic Holography, however this technique is out of the scope of this discussion.

The acoustic wave propagation in a continuous medium can be exactly represented by the Navier-Stokes equations. However, for noise levels observed in most of the daily and industrial applications (let's say below 130 dB), the acoustic wave propagation can be considered as linear and isentropic phenomena (see Pierce [11]). Therefore, the complex Navier-Stokes equations can significantly simplified into the (Helmholtz) wave equation and still accurately represent the acoustic wave propagation phenomena:

$$\left(\frac{1}{c_0^2}\frac{\partial^2}{\partial t^2} - \nabla^2\right) p = q(t)\delta(\mathbf{x} - \mathbf{x_0}), \tag{7}$$

where c_0 is the sound speed. In absence of sound sources, the right-hand side of the equation above is equal to zero. However, this equation becomes non-homogeneous in presence of an elementary monopole source described by $q(t)$. The Dirac Delta function $\delta(\mathbf{x} - \mathbf{x_0})$ provides the information about the geometrical location of the sound source. The non-homogeneous wave equation has the free-field (absence of reflections or solid boundaries) solution:

$$p(\mathbf{x}, \mathbf{x_0}, t) = \frac{1}{4\pi}\frac{q(\mathbf{x_0}, t - |\mathbf{x} - \mathbf{x_0}|/c_0)}{|\mathbf{x} - \mathbf{x_0}|}. \tag{8}$$

This solution informs some important aspects about the propagation of acoustic waves. Firstly, that the amplitude of the acoustic pressure decays inversely with the distance between source and observer ($|\mathbf{x} - \mathbf{x_0}|$). Secondly, that the acoustic pressure observed at a moment t is related with the source characteristics at a previous instant $|\mathbf{x} - \mathbf{x_0}| / c_0$. In order words, the information about the acoustic source propagates with finite speed c_0 in the medium. Therefore, a key concept for acoustic beamforming is the retarded time (t_0) formally defined as:

$$t_0 = \frac{|\mathbf{x} - \mathbf{x_0}|}{c_0}. \tag{9}$$

3.0 DELAY-AND-SUM BEAMFORMING

3.1 Time domain formulation

This section will introduce some fundamental concepts to the understanding of the beamforming technique. Those basic concepts are introduced together with the simplest and more robust beamforming approach, the Delay-and-Sum (DSB) technique [5, 14, 15]. This approach, schematically presented in Fig. 5, considers an *array* of m microphones and a *search grid* located in the plane where the noise source(s) are expected to be located. The noise localization procedure consists of:

1. define a plane where the noise source is expected to be located and divide this plane into a (rectangular) grid;

2. scan each grid node. For each node, the time signal measured by each microphone is delayed by the respective retarded time ($t_0 = |\mathbf{x} - \mathbf{x_0}| / c_0$);

3. the signal of each microphone is then summed and divided by the number of microphones (M) to generate the *beamformer output map*.

Following this procedure, if a source is present in the searching grid node, a constructive interference will occur and the final beamformer signal will be amplified. Otherwise, the phase mismatch will cancel the signal making the resulting amplitude will to be small, indicating the absence of sound source in that search grid position.
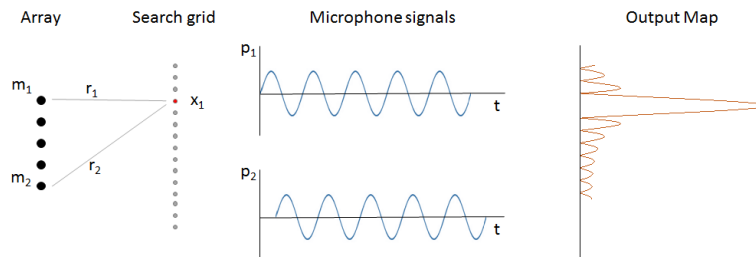

Figure 5: Delay-and-Sum Beamforming.

The beamformer output ($L(t)$) is mathematically expressed as:

$$L(t, \mathbf{x_0}) = \frac{4\pi}{M} \sum_{m=1}^{M} p_m \left(\mathbf{x_0}, t + t_0 \right) |\mathbf{x} - \mathbf{x_0}|, \tag{10}$$

where p_m is the signal measured by each microphone, M is the number of microphones, $\mathbf{x_0}$ is the source position and $\mathbf{x}$ is the microphone location.

3.2 Frequency domain formulation

The time domain is the simplest and computationally faster beamforming formulation. However, it cannot allow the application of complex post-processing and deconvolution techniques. The microphone data interpretation in the frequency domain allows the implementation complex calculation techniques and, consequently, improved results.

The frequency domain beamformer formulation starts with the free-field monopole solution (Eq. 8) Fourier-transform:

$$P(\mathbf{x}, \mathbf{x_0}, \omega) = \mathcal{F}\left\{(p(\mathbf{x_0}, t))\right\} = \int_{-\infty}^{\infty} p(\mathbf{x_0}, t) \, \mathrm{e}^{\mathrm{i}\,\omega\,\tau} \mathrm{d}\,\tau = \frac{Q(\omega)\mathrm{e}^{-\mathrm{i}\,\omega\,t_0}}{4\pi\,|\mathbf{x} - \mathbf{x_0}|}, \tag{11}$$

where ω is the angular frequency. The time delay (t_0) corresponding to the acoustic wave propagation distance between source and microphone is, now in the frequency domain, represented by the complex number $\mathrm{e}^{-\mathrm{i}\,\omega\,t_0}$.

The Fourier-transform of the beamformer presented in Eq. 10 is:

$$L(\omega, \mathbf{x_0}) = \mathcal{F}\left\{z(t)\right\} = \frac{4\pi}{M}\sum_{m=1}^{M} |\mathbf{x} - \mathbf{x_0}| \, P(\mathbf{x}, \mathbf{x_0}, \omega)\mathrm{e}^{-\mathrm{i}\,\omega\,t_0}$$

$$= \frac{1}{N}\sum_{m=1}^{N} s(\mathbf{x}, \omega)P(\mathbf{x}, \mathbf{x_0}, \omega), \tag{12}$$

where $s(\mathbf{x}, \mathbf{x}_0, \omega)$ is the so-called *steering function*:

$$s(\mathbf{x}, \mathbf{x}_0, \omega) = 4\pi\,|\mathbf{x} - \mathbf{x_0}|\,\mathrm{e}^{-\mathrm{i}\,\omega\,t_0}. \tag{13}$$

Considering an array with M microphones, the steering function can be summarized in the so-called *steering vector*:

$$g(\mathbf{x}, \omega) = \begin{pmatrix} 4\pi\,|\mathbf{x_1} - \mathbf{x_0}|\,\mathrm{e}^{-\mathrm{i}\,\omega\,t_1} \\ 4\pi\,|\mathbf{x_2} - \mathbf{x_0}|\,\mathrm{e}^{-\mathrm{i}\,\omega\,t_2} \\ \vdots \\ 4\pi\,|\mathbf{x_M} - \mathbf{x_0}|\,\mathrm{e}^{-\mathrm{i}\,\omega\,t_M} \end{pmatrix} \tag{14}$$

where $(\mathbf{x_1}\ldots\mathbf{x_M})$ represents the position of each microphone in the array and $(t_1\ldots t_M)$ is the propagation time between the searching grid point $\mathbf{x_0}$ and the respective microphone. In some occasions, the analyses become more convenient if the steering vector is normalized by the distance between source and microphone array center. Therefore, the normalized steering vector is defined as:

$$\hat{e}(\mathbf{x}, \omega) = \frac{g(\mathbf{x}, \omega)}{|\mathbf{x_c} - \mathbf{x_0}|} = \frac{1}{|\mathbf{x_c} - \mathbf{x_0}|}\begin{pmatrix} |\mathbf{x_1} - \mathbf{x_0}|\,\mathrm{e}^{-\mathrm{i}\,\omega\,t_1} \\ |\mathbf{x_2} - \mathbf{x_0}|\,\mathrm{e}^{-\mathrm{i}\,\omega\,t_2} \\ \vdots \\ |\mathbf{x_M} - \mathbf{x_0}|\,\mathrm{e}^{-\mathrm{i}\,\omega\,t_M} \end{pmatrix} \tag{15}$$

where $\mathbf{x_c}$ is the microphone array center position.

The Fourier-transformed microphone signals can also be presented in the vector format:

$$Y(\omega) = \begin{pmatrix} P_1(\omega) \\ P_2(\omega) \\ \vdots \\ P_M(\omega) \end{pmatrix} \tag{16}$$

therefore the beamformer $Z(\omega)$ can be represented in the matricial form as:

$$Z(\omega) = \frac{g(\mathbf{x}, \omega)^\dagger Y(\omega)}{M} \tag{17}$$

where $(\cdot)^\dagger$ notes the Hermite form of a vector (transpose and complex conjugated).

The power of the output signal can be calculated with $L(\mathbf{x}) = |Z|^2$. Since Z is complex:

$$L(\mathbf{x}) = Z\,Z^* \tag{18}$$
$$= (g^\dagger Y)(g^\dagger Y)^* \tag{19}$$
$$= g^\dagger (Y\,Y^\dagger)g \tag{20}$$

This brings to another very important concept in the beamforming theory that is the *Cross-Spectral Matrix* (CSM).

$$Y(\omega)\,Y(\omega)^\dagger = \text{CSM}(\omega) = \begin{pmatrix} Y_1 Y_1^* & \ldots & Y_1 Y_M^* \\ \vdots & \ddots & \vdots \\ Y_M Y_1^* & \ldots & Y_M Y_M^* \end{pmatrix} \tag{21}$$

with these concepts in mind, it is already possible to set a first application which allow us to analyze the strengths and limitations of the conventional beamforming technique. The conventional beamforming analysis will allow us to understand the importance of the deconvolution techniques.

3.3 Applications of the conventional beamforming technique

"Complicated sources" (nomenclature originally used by Brooks and Humphreys [16]) are used here to analyze the conventional beamforming technique. Brooks and Humphreys recognizes that spatially distributed and statistically correlated noise sources are more complex to be localized than statistically uncorrelated point sources. In real life applications, the aerodynamically generated noise is produced by a combination of sources that could be approximated to a point source, e.g. whistling a cavity(ies), which, in general are statistically uncorrelated sources, or a continuous source, e.g. the vortex-shedding noise produced by the flow passing by a sufficiently long cylinder, which has a relatively long spatial statistical correlation length, situation that represents an extra challenge to beamforming source localization.

The University of Twente's logo is adopted here to exemplify the beamforming technique application. This example uses 847 statistically uncorrelated, closely spaced point sources, schematically shown in Fig. 6, to construct the letters of the UTwente logo. All sources produce noise with the similar frequency of 6 kHz and amplitude of 100 dB (sound pressure level). The acoustic sources are localized considering the microphone array geometry shown in Fig. 3 facing the sources at 1.5 m distance. The acoustic sources localization is performed considering a rectangular search grid of 0.5 by 0.5 m^2 divided by 101 by 101 grid points with resolution of 0.01 by 0.01 m^2.
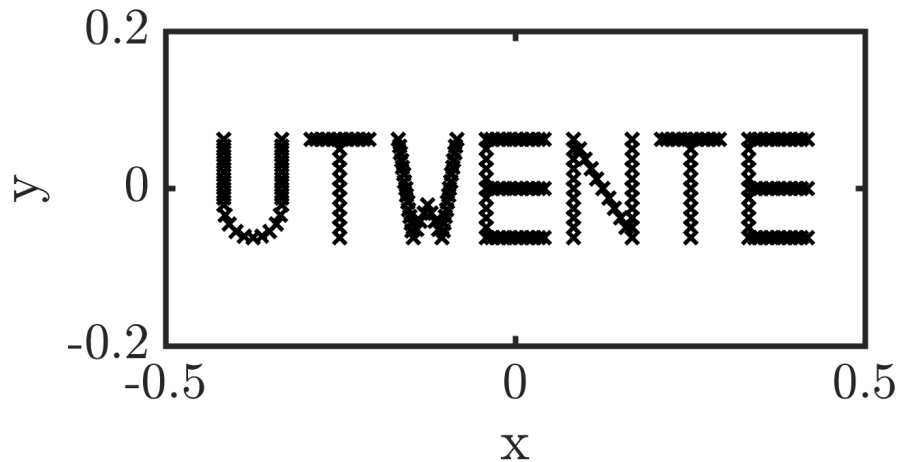
Figure 6: Localization of the closely located point sources adopted to simulate a continous source and evaluate the beamforming technique.

Figure 7 shows the noise sources localized with the conventional beamforming algorithm. This figure shows that within a dynamic range of 12 dB the conventional beamforming technique is able to localize the sources. However, it is noticed that the spatial resolution of this techniques is not optimal leading to many sources be seen as merged. Consequently, the amplitude of the located sources are significantly higher than the amplitude of the simulated sources. The source merging effect is more pronounced in letters which presents union of lines, such as T, E and specially the letter W (close to the center). This result shows the spatial resolution plays an important role in the beamforming technique. Furthermore, it is seen that the microphone array responds to the sound source "creating" pseudo sources of (relatively) small amplitude. In this case it is seen that the logo, presented in red, has amplitude of approximately 112 dB, while the background, presented in blue has amplitude of approximately 100 dB (the amplitude of the original sources). This effect of "creation" pseudo sound sources due to the microphone array geometry and the microphone array resolution are discussed in the next section where the microphone array *point-spread-function* is discussed.

3.4   The Point-Spread-Function (PSF)

The microphone array consists of a number of individual sensors having a certain spatial distribution. Considering the practically impossibility of having a spatially continuous distribution of sensors, it is expected that the microphone array will work as a spatial filter bank. The properties of those filters are essential to determine the microphone array performance interfering in the localizing and quantification of acoustic sources. In beamforming theory, the *Point-Spread-Function* (PSF) determines how a given microphone array responds to a point monopole placed in front of the array.

An ideal microphone array would respond to a monopole point source showing a infinitesimally small point source output and without creating "pseudo" sound sources. However, the finite microphone array size and the discontinuous distribution of microphones makes any real microphone array to spatially alias the point source and contaminate the beamforming output map with side lobes which are seen as "pseudo" sound sources. Underbrink [17] recommends that the minimum microphone array distance does not exceed half of the acoustic wavelength to avoid significant spatial aliasing, furthermore a large number of studies are present in literature proposing different array geometries which minimize the side-lobe formation.
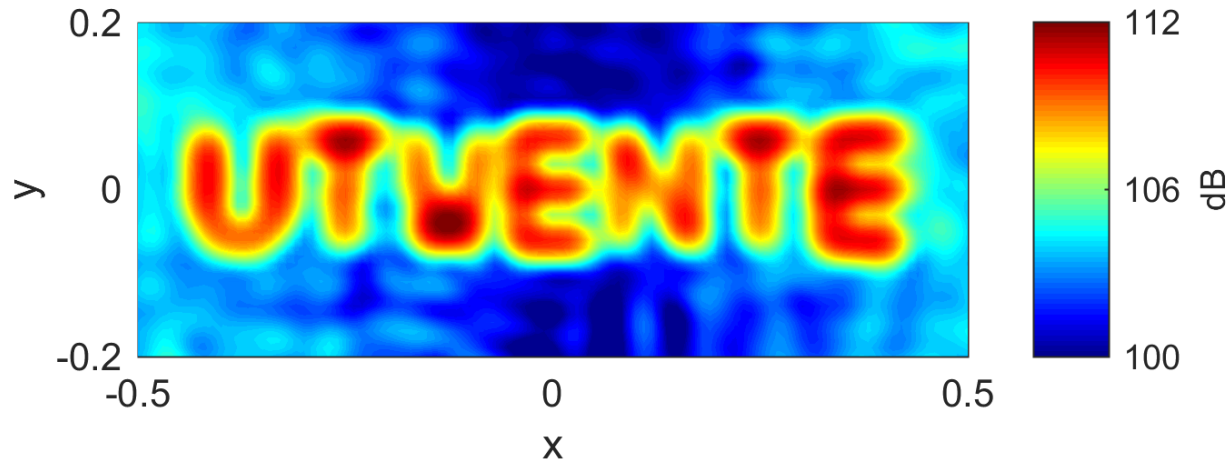
Figure 7: UTwente logo beamformed with the conventional beamforming technique.

The PSF function provides insightful information regarding the array performance, providing the beam width and the main-to-side-lobe ratio (MSR). In real applications, the beamforming output map is always convolved with the microphone array response and therefore it is called *dirty map*.

The knowledge of array the PSF gives information about the the "transfer function" of the microphone array for a given point source which is instrumental to the application of deconvolution techniques to be discussed in the following sections.

3.5 The convolution between the acoustic sources and the microphone array PSF

The raw image taken by a photo camera, a microscope, a telescope or an acoustic camera brings the sensor response convolved with the actual image. Photo cameras, for example, can reduce the sensor influence by increasing the number of pixels and reducing the spacing between them and by improving the lenses quality. By enhancing the hardware the camera PSF is enhanced resulting into a larger MSR and minimum bandwidth.

By turn, for an acoustic array – also known as *acoustic camera* –, it is possible to improve the microphones distribution up to a certain optimum or increase the number of microphone sensors up to the budget limit and/or the data acquisition and logging system capacity. Due to those practical constraints, researchers have invested large efforts to develop deconvolution algorithms which could solve these problems through a much more affordable and practical way. In signal and image processing, the concept of deconvolution is widely used. The deconvolution principle assumes that a recorded signal or image (h) is a convolution of the actual image (f) and a certain transfer function (g) which represents the array response to a given source – in acoustic beamforming this is the array PSF:
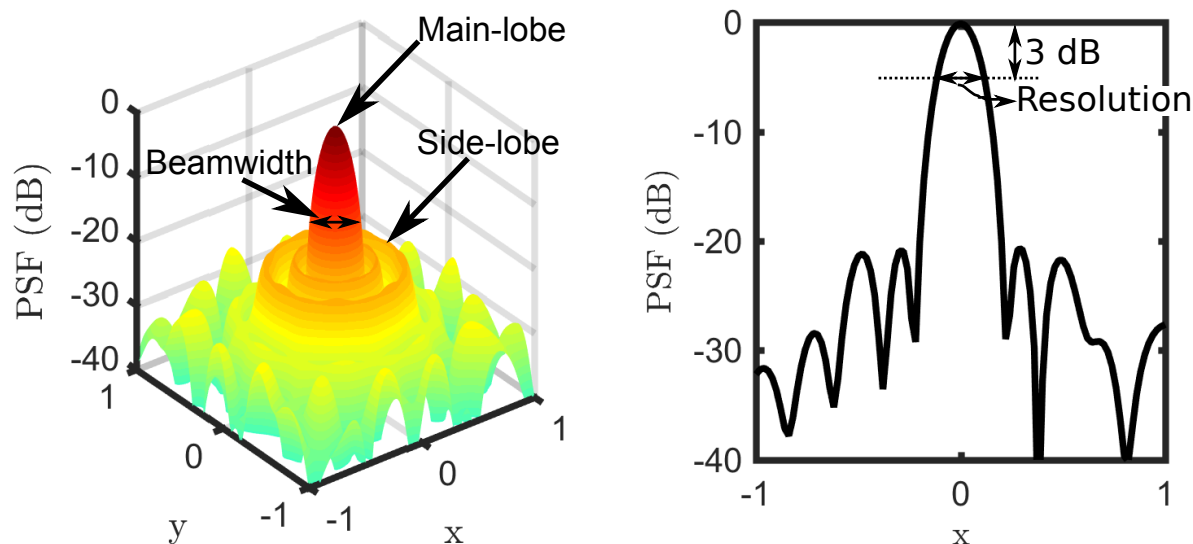
$$h = f \star g \tag{22}$$

Figure 8: Schematic representation of a typical Point-Spread-Function. The array resolution is defined by the beam width at a position 3 dB lower compared to the peak. This indicates the maximum spatial resolution of a microphone array. The array main to side-lobe ratio indicates the capacity of a array distinguish sources of different amplitudes.

where $\star$ represent the convolution operator.

Crystal clear images of planets and stars could be obtained through the application of deconvolution techniques to the raw "dirty image" f. This example is more clearly seen by the "dirty image" acquired by the Hubble telescope and the post-processed (through the knowledge of the telescope PSF function g of this telescope) image, see Fig. 9.
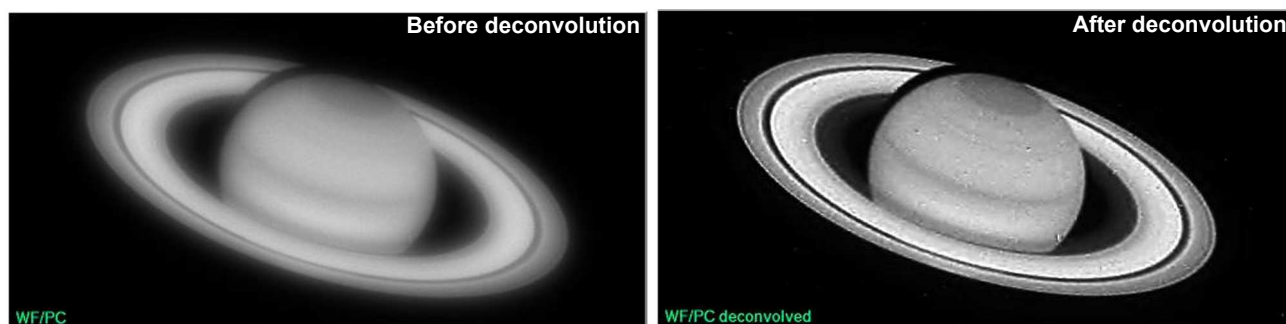

Figure 9: Hubble Space Telescope photos of Saturn taken before and after convolution. Source: [18]

3.6   Quantification of results

In the engineering analysis of noise reduction solutions the localization of acoustic sources can provide qualitative indication of the most important noise sources, however the quantification will provide actual means to engineers perform complex design decisions.

From the theoretical point of view, the source quantification with conventional beamforming represents the most complex task due to the fact that the sources distribution is intrinsically convoluted with the source map $L(\mathbf{x})$. Even with application of advanced deconvolution techniques, the precise quantification of sources, in complex environments, still challenge state-of-the-art researchers. However, reliable noise source quantification are possible if certain conditions are satisfied. Assuming a distribution of incoherent sources $q(\mathbf{x_0})$, Dougherty [19] proposed that the source map can be written as the sources and array PSF convolution:

$$L(\mathbf{x}) = \int_{\mathbf{x} \in \mathcal{G}} q(\mathbf{x_0}) \text{PSF}(\mathbf{x}, \mathbf{x_0}) \mathrm{d}\mathbf{x}, \tag{23}$$

therefore the absolute source pressure levels can be extracted from the "dirty map" ($L(\mathbf{x})$) if the constraints are satisfied:

- the localized sources are incoherent point sources;

- in the array direction, the sources have uniform directivity

- the beamformer spatial resolution is high enough to distinguish different sources;

- the distance between sources are large enough to avoid the interference of side-lobes;

- the noise measured by all array microphones is coherent;

- there are absence of reflections;

Those are very difficulty conditions to be satisfied in actual (wind tunnel) tests. Therefore, Brooks and Humpphreys [20] propose a two steps procedure for quantitative determination of sound sources: First the source map is integrated and later the integral is normalized to consider the width of the PSF of the beamformer:

$$L_f(\mathbf{x}) = \left(\int_{\mathbf{x} \in \mathcal{G}} L(\mathbf{x}) \mathrm{d}\mathbf{x} \right) \left(\frac{P_{\text{SIM}}}{\int_{\mathbf{x} \in \mathcal{G}} L_{\text{SIM}}(\mathbf{x}) \mathrm{d}\mathbf{x}} \right) \tag{24}$$

where $L_f(\mathbf{x})$ represents the normalized source pressure, $L_{\text{SIM}}(\mathbf{x})$ is the beamforming source map, P_{SIM} is the simulated beamforming source pressure and $\mathcal{G}$ represents the searching grid domain. This approach has been extensively tested and proven of good accuracy provided that the full CSM matrix is used, i.e. no diagonal removal is considered. The diagonal removal technique is shown to provide less reliable quantification results.

4.0 DECONVOLUTION TECHNIQUES

4.1 DAMAS

In 2004, Brooks and Humphrey [16] proposed the Deconvolution Approach for the Mapping of Acoustic Sources (DAMAS) method aiming "demystify the 2D and 3D arrays results, to reduce misinterpretation, and to more accurately quantify position and strength of aeroacoustic sources".

The key idea behind DAMAS is to *model* the CSM considering a distribution of *statistically independent* sources placed in the search grid. The modeled CSM is then compared to the measured CSM and a linear system of equations is formed. The solution to this system of equations provides the source intensity and location.

DAMAS initially proposes to consider the source amplitude Q_n normalized by a "virtual" microphone placed a given reference position (e.g. the center of the microphone array) due to a source placed in a position n of the searching grid:

$$P(\omega) = Q_n(\omega)e^{-1}_{m:n}(\mathbf{x}, \omega),$$

(25)

where $e_{m:n}$ is one element of the normalized steering vector, defined in Eq. 15, linking the microphone m to a position n in the searching grid. The pressure cross-power is then written as:

$$P_{m:n}(\omega)P^*_{m:n}(\omega) = (Q_n(\omega)e^{-1}_{m:n}(\mathbf{x}, \omega))^*(Q_n(\omega)e^{-1}_{m:n}(\mathbf{x}, \omega)) = Q_n(\omega)Q^*_n(\omega)(e^{-1}_{m:n}(\mathbf{x}, \omega))^*(e^{-1}_{m:n}(\mathbf{x}, \omega)),$$

(26)

therefore the *modeled* CSM considering a single source placed in a position of the searching grid n is:

$$CSM^{mod}_n(\omega) = X_n \begin{bmatrix} (e^{-1}_1)^*(e^{-1}_1) & \cdots & (e^{-1}_1)^*(e^{-1}_M) \\ \vdots & \ddots & \vdots \\ (e^{-1}_M)^*(e^{-1}_1) & \cdots & (e^{-1}_M)^*(e^{-1}_M) \end{bmatrix}_n,$$

(27)

where $X_n = P(\omega)P^*(\omega)$ is the microphone power-spectral density contribution of a source located at the grid position n normalized to the level of a microphone localized in $r_m = r_c$. Now considering that all sources placed in the search grid are statistically incoherent, the modeled CSM can be written as the sum of all contributions:

$$CSM^{mod}(\omega) = \sum_{n=1}^{N} CSM^{mod}_n(\omega)$$

(28)

where N is the total number of points in the searching grid. Similarly to Eq. 20, with the $CSM^{mod}(\omega)$ it is possible to compute the modeled beamforming output power for a given position n in the searching grid as:

$$L^{mod}(\mathbf{x}) = \left[\frac{\hat{e}^T CSM^{mod}(\omega)\hat{e}}{M^2} \right]_n$$

(29)

and

$$L^{mod}(\mathbf{x}) = \frac{\hat{e}^T_n \sum_{k=1}^{N} X_k [\,]_k \hat{e}_n}{M^2} = \sum_{k=1}^{N} \frac{\hat{e}^T_n [\,]_k \hat{e}_n}{M^2} X_k$$

(30)

where the bracketed term is that of Eq. 27 therefore the beamforming output map is summarized as:

$$L^{mod}(\mathbf{x}) = \sum_{k=1}^{N} A_{nk} X_k$$

(31)

where

$$A_{nk} = \frac{\hat{e}^T_n [\,]_k \hat{e}_n}{M^2}$$

(32)

By equating an $L^{mod}(\mathbf{x})$ with the conventional beamforming processed $L(\mathbf{x})$ from measured data, we have a linear system of equations:

$$\hat{Y} = \hat{A}\hat{X}$$

(33)

where $\hat{A}$, $\hat{X}$ and $\hat{Y}$ have components A_{nk}, X_k and $L(\mathbf{x})$, respectively.

The matrix $\hat{A}$ is square of size $N \times N$ and if it was a non-singular matrix, it could be simply inverted providing the source strengths as $X = \hat{A}^{-1}\hat{Y}$. However, for practical applications, the matrix $\hat{A}$ is non-singular with very low rank (number of independent equations). Classical techniques for inversion of low rank matrices such as Single Value Decomposition (SVD) and Conjugate Gradient Methods (CGM) produce nonsensical results even for very simple sources. Therefore Brooks and Humphrey proposed a tailored iterative method to solve the problem. Considering a single equation of the linear system:

$$A_{n1}X_1 + \cdots + A_{nk}X_n + \cdots + A_{nN}X_N = Y_n \tag{34}$$

where n and k are grid point index numbers of the search grid. With A_{nn}=1, Eq 34 is written as:

$$X_n = Y_n - \left[\sum_{k=1}^{n-1} A_{nk}X_k + \sum_{k=n+1}^{N} A_{nk}X_k\right] \tag{35}$$

this equation is implemented in an iterative algorithm to find the source strength distribution X_n in the search grid points:

$$X_1^{(i)} = Y_1 - \left[0 + \sum_{k=1+1}^{N} A_{1k}X_k^{(i-1)}\right]$$

$$X_n^{(i)} = Y_n - \left[\sum_{k=1}^{n-1} A_{nk}X_k^{(i)} + \sum_{k=n+1}^{N} A_{nk}X_k^{(i-1)}\right] \tag{36}$$

$$X_N^{(i)} = Y_N - \left[\sum_{k=1}^{N-1} A_{Nk}X_k^{(i)} + 0\right]$$

Brooks and Humphrey propose that, for the first iteration, the values of X_n should be taken as zero. Furthermore, since the source strengths are always larger than zero, a positive constraint on X_n is enforced to ensure stability of the system. After all grid points have been completed in an iteration, the calculation is reversed moving from $n = N$ back to $n = 1$ to smooth the iteration steps.

The DAMAS algorithm requires a high number of calculations that makes this a very time consuming algorithm. In general, the computational time for each iteration depends only on the number of grid points. Accordingly to Brooks and Humphrey, the time per iteration can be expressed by time $= C(2N)^2$, in which C is a hardware dependent constant. Figure 10 shows the UTwente logo beamformed with 500 iterations of the DAMAS algorithm. This figure shows that the DAMAS algorithm clearly finds the sources in the logo and it much less subject to the influence of the side-lobes when compared with results calculated by the conventional beamforming algorithm. The source amplitude is much closer to the original 100 dB imposed in the simulations, indicating that the spatial resolution of this algorithm is also much better, compared to conventional beamforming. Few pseudo-sources due to the influence of the array side-lobes are located.

4.2 DAMAS2

The DAMAS algorithm represented a remarkable advance in the application of microphone array techniques. However, this approach requires the PSF computation for each point of the searching grid that significantly adds computational cost limiting, therefore, its use in engineering applications. Aiming accelerate the computational process and present improved results, relative to the conventional beamforming technique, Dougherty proposed in 2005 the DAMAS2 [19] algorithm.
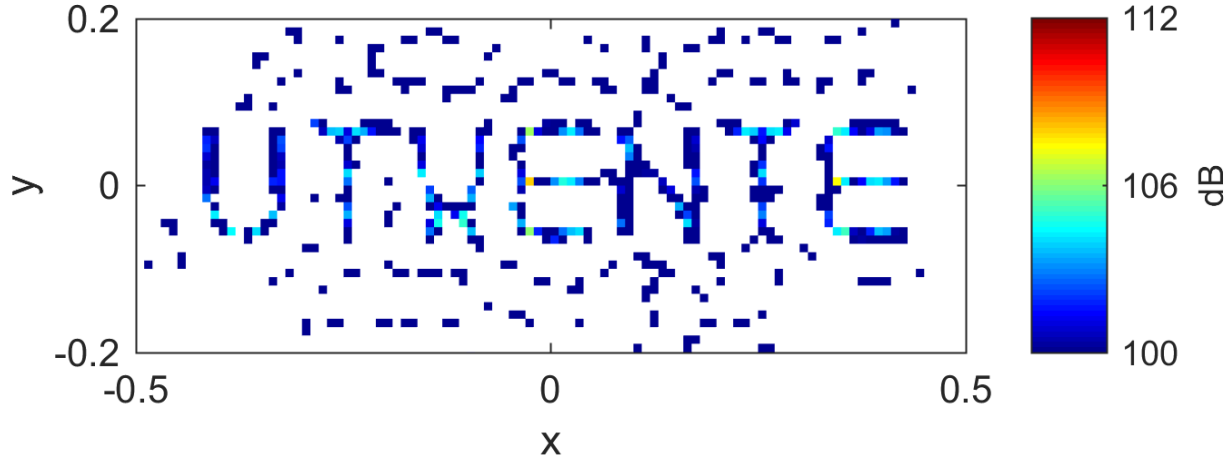
Figure 10: UTwente logo beamformed with 500 iterations of the DAMAS algorithm.

The DAMAS2 algorithm computes the convolution between the microphone array PSF and the sources in the Fourier domain. This significantly improves the calculation speed and contributes to solve a limitation of the DAMAS algorithm. The algorithm DAMAS does allow the implementation of a regularization technique to control the amplification of high-frequency noise, which may eventually happen in case of excessively refined grids. DAMAS2, by turn, adds regularization by proposing the application of a low-pass filter preventing the acoustic image become too noisy in the eventual situation where the searching grid is finer than the array resolution can support.

Similarly to DAMAS, DAMAS2 considers that the "dirty map" $L(\mathbf{x})$ is written as a convolution of the array PSF and the source. This formulation is repeated here for clarity as:

$$L(\mathbf{x}) = \int_{\mathbf{x} \in \mathcal{G}} \text{PSF}(\mathbf{x}, \mathbf{x_0}) q(\mathbf{x_0}) \mathrm{d}\mathbf{x_0} \tag{37}$$

Similarly to DAMAS, the calculation of the deconvolution requires the assumption of incoherent distribution of sources. In the DAMAS algorithm, the computation of the PSF is the most time consuming step. Therefore Dougherty proposes the use of a *shift-invariant* PSF to simplify the calculations. The shift-invariant PSF depends only of the distance $\mathbf{x} - \mathbf{x_0}$ between the search grid point and the source. Therefore, the shift-invariant PSF can be written as:

$$\text{PSF}(\mathbf{x}, \mathbf{x_0}) = \text{PSF}(\mathbf{x} - \mathbf{x_0}). \tag{38}$$

No PSF fulfills the shift-invariant conditions, therefore Dougherty proposes to assume an approximate PSF which is representative of a source located in the center of the search grid. Using a shift-invariant PSF, Eq 37 is written as:

$$L(\mathbf{x}) = \int_{\mathbf{x} \in \mathcal{G}} \text{PSF}(\mathbf{x} - \mathbf{x_0}) q(\mathbf{x_0}) \mathrm{d}\mathbf{x_0}. \tag{39}$$

Assume a shift-invariant PSF is generally a good approximation in situations where the source region is small compared to the distance between the sound source and array. The output map formulation of Eq. 39 can be algebraically written as a linear system of equations $Y = AX$, where the solution $X = A^{-1}Y$ has the matrix inversion process facing the same singularity problems as DAMAS. Therefore, Dougherty proposes the DAMAS2 for noise source localization:

1. Compute the source map spatial Fourier transform: $\tilde{p}(\mathbf{k}) = \text{FFT}[\text{PSF}(\mathbf{x})]$, where $\mathbf{k}$ is the spatial PSF wavenumber;

2. Set the PSF normalization parameter $a = \sum_{\mathbf{x}} |PSF|$;

3. Initialize the solution $q(\mathbf{x}) = 0$ for each point $\mathbf{x}$ in the searching grid;

4. Iterate until convergence:

   (a) Apply the spatial Fourier transform to the sources distribution: $\tilde{q}(\mathbf{k}) = \text{FFT}[q]$;

   (b) Apply the Gaussian spatial filter in order to remove eventual noise due to excessively fine searching grid: for each $\mathbf{k}$, scale $\tilde{q}(\omega)$ by $\exp(-k^2/(2k_c^2))$ (where k_c is the spatial cut-off frequency for the Gaussian regularization);

   (c) In the Fourier domain, compute the convolution between the sources amplitude ($\tilde{q}(\vec{k})$) and the microphone array PSF ($\tilde{p}(\mathbf{k})$): $\tilde{r}(\mathbf{k}) = \tilde{p}(\mathbf{k})\tilde{q}(\vec{k})$ for each $\mathbf{k}$;

   (d) Apply the inverse Fourier transform to calculate the "new" dirty map, which represents the convolution between the calculated sources and the microphone array PSF: $r(\mathbf{x}) = \text{iFFT}[\tilde{r}(\vec{k})]$;

   (e) Update the source amplitude: $q^{(i+1)}(\mathbf{x}) = q^{(i)}(\mathbf{x}) + [L(\mathbf{x}) - r(\mathbf{x})]/a$ for each $\mathbf{x}$;

   (f) Replace each negative value of $q(\mathbf{x})$ by 0.

The DAMAS2 algorithm considerably reduces the execution time since, each iteration, requires the calculation of a single Fourier transform and its inverse. The cut-off frequency k_c is a "tweaking" parameter chosen to optimize the visual and quantitative representation of the acoustic image.

Figure 11 shows the UTwente logo beamformed now with help of the 500 iterations of the DAMAS2 algorithm. The shift-invariant PSF assumed in DAMAS2 accelerates significantly this algorithm computation. While DAMAS consumes more than 25 hours to compute the results, the DAMAS2 algorithm consumes no more than a couple of minutes. However, some differences in the results are noticed. When compared to DAMAS, the spatial resolution with DAMAS2 is compromised, showing sources with amplitude close to 112 dB in the letters T, W and E. Furthermore, the side-lobes influence are much more pronounced noticed by the presence of some pseudo sources localized out of the actual source region due to invalidity of the shift invariant PSF in the outer region of the search grid.

4.3 CLEAN-PSF

The CLEAN-PSF is presented as a building block to understand the CLEAN-SC algorithm. Astronomers widely use the CLEAN algorithm to perform deconvolution of telescope and radio-telescope images and therefore localize, specially, less bright stars closely located to a very bright stars. The CLEAN-PSF algorithm also considers that the "dirty map" represents a convolution between the actual source distribution and the array PSF. The CLEAN-PSF algorithm iteratively finds the highest source value in the "dirty map" and then subtracts the contribution of this source from the "dirty map". The found sources are stored in a separate "clean map"
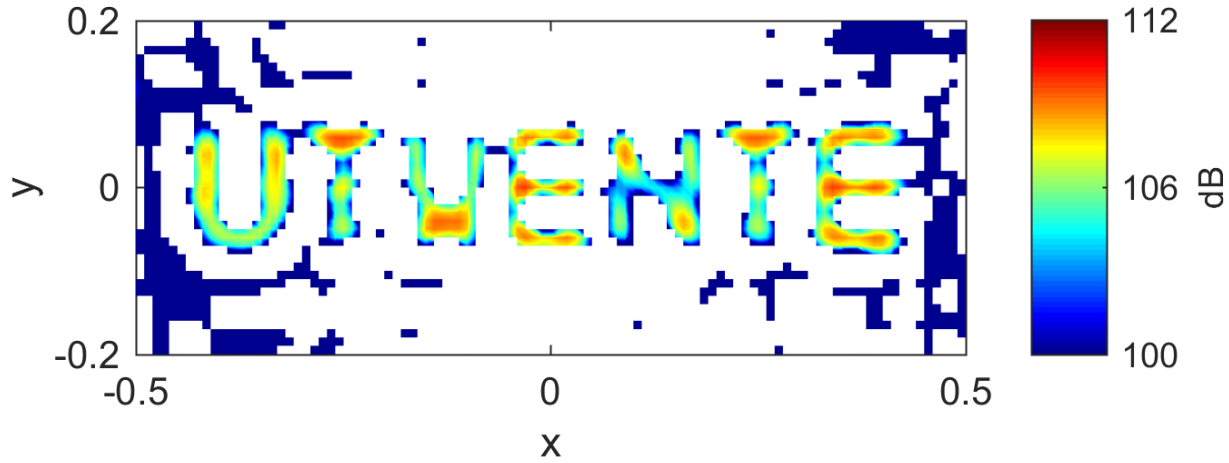
Figure 11: UTwente logo beamformed with 500 iterations of the DAMAS2 algorithm.

and the source contribution is removed from the CSM, creating therefore a degraded CSM. The CLEAN-PSF method assumes that the source plot is composed of PSFs, e.g. each node in the searching grid has it's own PSF. In essence, the CLEAN-PSF algorithm iterates as following [21]:

1. obtain the "dirty map" with conventional beamforming;

2. search for the peak location in the dirty map;

3. subtract the appropriately scaled PSF from the dirty map;

4. replace this PSF by a "clean beam".

The derivation of the CLEAN-PSF algorithm considers the space S composed by the indexes (m, n) used to refer to the microphones m and n in the array. The approach defines the weight vector is defined as:

$$\mathbf{w} = \frac{g}{\left(\sum_{(m,n)\in S} |g_m|^2 \, |g_n|^2 \right)^{1/2}} \, , \tag{40}$$

that represents the proportional contribution of each steering vector regarding the sum of the "length" of all steering vectors. Following this definition, the output map is written as:

$$L = \mathbf{w}^\dagger CSM \mathbf{w} \, , \tag{41}$$

using this notation, the CSM induced by a source of unitary amplitude placed in the searching grid position of index j is:

$$CSM_j = g_j g_j^\dagger \, . \tag{42}$$

The conventional beamforming technique finds the unitary source power as:

$$L = \mathbf{w}^\dagger \left[g_j g_j^\dagger \right] \mathbf{w} \,, \tag{43}$$

the Point Spread Function (PSF) definition is restated above to maintain clarity and keep the notation consistent with the rest of this section.

The CLEAN-PSF method iteratively searches for the sources. In the first step, $i = 0$, the "degraded" CSM (D) is initialized by the measured CSM:

$$\mathbf{D}^{(i)} = \mathbf{D}^{(0)} = CSM \,. \tag{44}$$

The "dirty map" is calculated by conventional beamforming and the peak source location $\xi_{\text{max}}^{(i)}$ is determined. The CSM induced by the peak source in $\xi_{\text{max}}^{(i)}$ is given by

$$\mathbf{G}^i = P_{\text{max}}^{(i-1)} \mathbf{g}_{\text{max}}^{(i)} \mathbf{g}_{\text{max}}^{\dagger(i)} \,, \tag{45}$$

where $\mathbf{g}_{\text{max}}^{(i)}$ is the steering vector associated with the location $\xi_{\text{max}}^{(i)}$.

In the following step, the contribution of this peak source is removed from the "dirty map":

$$P_j^{(i)} = P_j^{(i-1)} - \mathbf{w}_j^\dagger \mathbf{G}^{(i)} \mathbf{w}_j \,. \tag{46}$$

Therefore equation is rewritten in terms of the steering vector as:

$$P_j^{(i)} = P_j^{(i-1)} - P_{\text{max}}^{(i-1)} \mathbf{w}_j^\dagger \left[\mathbf{g}_{\text{max}}^{(i)} \mathbf{g}_{\text{max}}^{\dagger(i)} \right] \mathbf{w}_j \,, \tag{47}$$

and the "clean" beam associated with $\xi_{\text{max}}^{(i)}$ is stored in the "clean" map is:

$$Q_j^{(i)} = P_{\text{max}}^{(i-1)} \Phi(\vec{\xi}_j - \vec{\xi}_{\text{max}}^{(i)}) \tag{48}$$

where Φ is a normalized clean beam of maximum value $\Phi(0) = 1$:

$$\Phi\left(\vec{\xi}_j - \xi_{\text{max}}^{\vec{(i)}} \right) = 10^{-\lambda \left| \vec{\xi}_j - \xi_{\text{max}}^{\vec{(i)}} \right|} \,. \tag{49}$$

the clean beam shape determines the source appearance in the "clean map". The Gaussian formulation will represent an spatially extended source as a single (concentrated) punctual source. In cases where the source has long spatial correlation length, e.g. airfoil trailing edge noise or vortex shedding behind a cylinder, this may lead to the source concentration into a point and eventual "visual" misinterpretation of the results. It is important to keep in mind that the clean beam shape is an source visualization artifact. The spatially distributed actual source will have its intensity concentrated in this "clean beam", therefore the correct source amplitude is retrieved by integration of the "clean beam".

To complete the iteration, the degraded CSM (D) is updated with the subtraction of the component $\mathbf{G}^i$ corresponding to the contribution to the CSM of a source induced by the peak source localized in $\xi_{\text{max}}^{(i)}$:

$$\begin{aligned} \mathbf{D}^{(i)} &= \mathbf{D}^{(i-1)} - \mathbf{G}^i \\ &= \mathbf{D}^{(i-1)} - P_{\text{max}}^{(i-1)} \mathbf{g}_{\text{max}}^{(i)} \mathbf{g}_{\text{max}}^{\dagger(i)} \,. \end{aligned} \tag{50}$$

The updated source power map is computed from the degraded CSM:

$$P_j^{(i)} = \mathbf{w}_j^{\dagger} \mathbf{D}^{(i)} \mathbf{w}_j \tag{51}$$

After all iterations are complete, the source map is written as the contribution of each clean beam plus the remaining degraded source map:

$$A_j = \sum_{i=1}^{I} Q_j^{(i)} + P_j^{(I)} \tag{52}$$

A stop criterion is set when the degraded CSM contains more information than in the previous iteration:

$$\| \mathbf{D}^{(i+1)} \| \leq \| \mathbf{D}^{(i)} \| \tag{53}$$

Figure 12 shows the UTwente logo beamforming map computed with CLEAN-PSF algorithm. Due to the statistical uncorrelation between sources and the spatial high concentration, the CLEAN-PSF algorithm is unable to recreate the line source distribution. The finite spatial resolution of the microphone array induces this algorithm to merge closely spaced sources into single larger sources. Therefore, the found sources have larger amplitude than those simulated. The large number of uncorrelated and spatially close sources leads this algorithm to create exaggerated large PSF's, with side-lobe contributions, which summed, result into large "pseudo sources" noticed in the map.
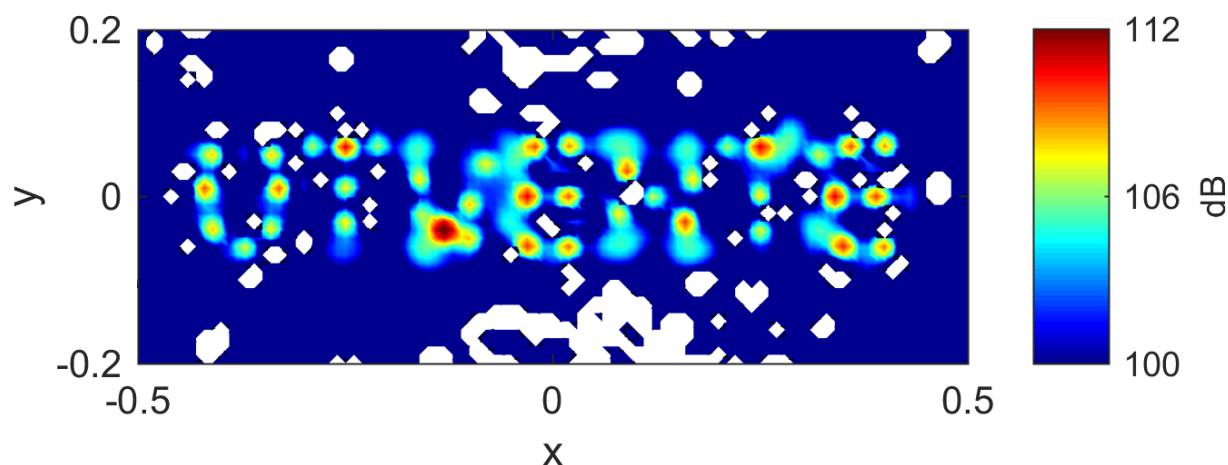

Figure 12: UTwente logo beamformed with 500 iterations of the CLEAN-PSF algorithm.

The array resolution effect and the side-lobe influence can be noticed if the source frequency is increased. Since the microphone array main-lobe to side-lobe ratio is proportional to the frequency and array the resolution inversely decays with frequency, Fig. 13 shows that the CLEAN-PSF capacity to localize the sources

significantly improves when the source frequency grows from 6 kHz to 20 kHz. Noteworthy is that the array adopted in this example has minimum distance between microphones much larger than the acoustic wavelength when the source frequency is 20 kHz. Therefore, the spatial alias results into a source with amplitude largely underestimated.

Figure 13: UTwente logo beamformed with CLEAN-PSF algorithm and source frequency of 20 kHz.

The number of incoherent sources and spatial concentration adopted in this simulation is much larger than the practical values found in experimental applications. Therefore, the situation discussed here represents a very complex case where the limits of this beamforming technique are tested.

4.4 CLEAN-SC

The deconvolution algorithms DAMAS, DAMAS2 and CLEAN-PSF assume that the source maps are composed by the convolution of PSFs and sources. Therefore, deconvolution is only possible in case of statistically uncorrelated sources. However, actual sources observed in aeroacoustic applications are not necessarily infinitesimal length point sources. Furthermore, they typically present non-negligible level of spatial correlation. The deconvolution methods DAMAS, DAMAS2 and CLEAN-PSF assume that the sources behave as monopoles with negligible directivity effects, at least, in the microphone array direction. This hypothesis is not necessarily true in large scale wind tunnel tests, in wind turbine noise measurements or aircraft fly-over tests. To overcome these limitations Pieter Sijtsma [21] proposed in 2007 the CLEAN-SC method inspired in the CLEAN-PSF methodology, broadly applied in astronomy. This approach assumes that the side lobes of a source map are coherent with the main lobe.

To overcome the requirement of spatially uncorrelated sources, the CLEAN-SC algorithm writes the source

cross-power of two spatially distinct sources localized in the grid points with indexes j and k as:

$$B_{jk} = \mathbf{w}_j^\dagger CSM \mathbf{w}_k \, . \tag{54}$$

Following this formulation, the degraded CSM matrix $\mathbf{D}^{(i)}$ is written in terms of the spatial correlation of the peak source, with location $\vec{\xi}_{\max}^{(i)}$, contribution $\mathbf{G}^{(i)}$ for every point of the search grid:

$$\mathbf{w}_j^\dagger \mathbf{D}^{(i-1)} \mathbf{w}_{\max}^{(\mathbf{i})} = \mathbf{w}_j^\dagger \mathbf{G}^{(i)} \mathbf{w}_{\max}^{(i)}, \text{ for all possible } \mathbf{w}_j \, . \tag{55}$$

This equation is satisfied when

$$\mathbf{D}^{(i-1)} \mathbf{w}_j^{(i)} = \mathbf{G}^{(i)} \mathbf{w}_{\max}^{(i)} \, . \tag{56}$$

This analysis, when compared to CLEAN-PSF, remains identical. However a different definition of $\mathbf{G}^{(i)}$ is used:

$$\mathbf{G}^{(i)} = P_{\max}^{(i-1)} \mathbf{h}^{(i)} \mathbf{h}^{\dagger(i)} \, , \tag{57}$$

where:

$$\mathbf{h}^{(i)} = \frac{\mathbf{D}^{(i-1)} \mathbf{w}_{\max}^{(i)}}{P_{\max}^{(i-1)}} \, , \tag{58}$$

therefore the degraded source map is written as:

$$
\begin{aligned}
P_j^{(i)} &= P_j^{(i-1)} - \mathbf{w}_j^\dagger \mathbf{G}^{(i)} \mathbf{w}_j \\
&= P_j^{(i-1)} - P_{\max}^{(i-1)} \mathbf{w}_j^\dagger \mathbf{h}^{(i)} \mathbf{h}^{\dagger(i)} \mathbf{w}_j \\
&= P_j^{(i-1)} - P_{\max}^{(i-1)} \mathbf{w}_j^\dagger \frac{\mathbf{D}^{(i-1)} \mathbf{w}_{\max}^{(i)}}{P_{\max}^{(i-1)}} \frac{\mathbf{w}_{\max}^{\dagger(i)} \mathbf{D}^{(i-1)}}{P_{\max}^{(i-1)}} \mathbf{w}_j \\
&= P_j^{(i-1)} \left[1 - \frac{\left| \mathbf{w}_j^\dagger \mathbf{D}^{(i-1)} \mathbf{w}_{\max}^{\dagger(i)} \right|^2}{P_j^{(i-1)} P_{\max}^{(i-1)}} \right] \\
&= P_j^{(i-1)} \left[1 - \frac{\left| \mathbf{w}_j^\dagger \mathbf{D}^{(i-1)} \mathbf{w}_{\max}^{\dagger(i)} \right|^2}{\left(\mathbf{w}_j^\dagger \mathbf{D}^{(i-1)} \mathbf{w}_j^{(i)} \right) \left(\mathbf{w}_{\max}^\dagger \mathbf{D}^{(i-1)} \mathbf{w}_{\max}^{(i)} \right)} \right] \, ,
\end{aligned}
\tag{59}
$$

where

$$\gamma = \left[1 - \frac{\left| \mathbf{w}_j^\dagger \mathbf{D}^{(i-1)} \mathbf{w}_{\max}^{\dagger(i)} \right|^2}{\left(\mathbf{w}_j^\dagger \mathbf{D}^{(i-1)} \mathbf{w}_j^{(i)} \right) \left(\mathbf{w}_{\max}^\dagger \mathbf{D}^{(i-1)} \mathbf{w}_{\max}^{(i)} \right)} \right]^\dagger \, , \tag{60}$$

can be interpreted as the source spatial correlation.

Figure 14 shows the UTwente logo beamfomed now with the CLEAN-SC algorithm. Similar to CLEAN-PSF, CLEAN-SC has difficulties to localize high number of spatially concentrated and statistically uncorrelated sources. A problem like this, with such number of perfectly uncorrelated sources, e.g. negligible correlation

length, is quite unlikely to be found in real engineering applications. This simulation case pushes the algorithm to the limit. The CLEAN-SC is widely recognized as a state-of-the-art algorithm applied to the noise sources localization and quantification.

Similarly to CLEAN-PSF, in this situation, all sources have exactly same amplitude and are physically spaced a distance much smaller than the array resolution. Therefore, the CLEAN-SC algorithm has difficulties to find the source of largest amplitude. For instance, when the source is located, the algorithm tends to merge closely spaced sources into a single source of larger amplitude.
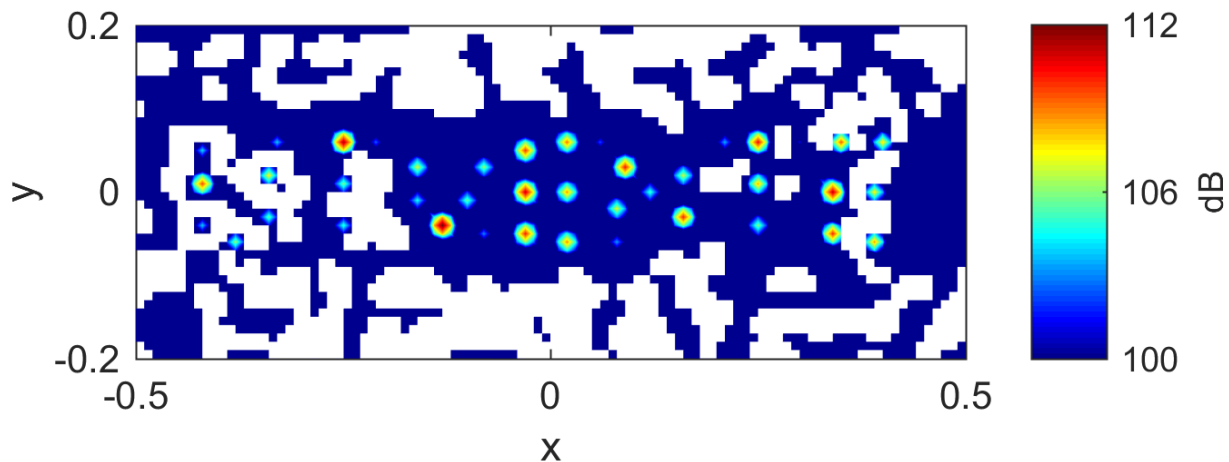

Figure 14: UTwente logo beamformed with CLEAN-SC algorithm.

Remembering that higher frequency results into positive effects to the source localization due to the enhancement of the microphone array main to side lobe ratio and better spatial resolution. Therefore, Fig. 15 show results when the source frequency is 20 kHz. In this case more sources are located, however letters such as N are almost completely missing. Similarly, the CLEAN-PSF case, the minimum distance betwen microphone pairs in the array imposes a spatial aliasing leading to remarkable reduction in the source levels determination.

ACKNOWLEDGMENTS

REFERENCES

[1] Herr, M. and Dobrzynski, W., "Experimental Investigations in Low Noise Trailing Edge Design," 10th *AIAA/CEAS Aeroacoustics Conference*, 2004.
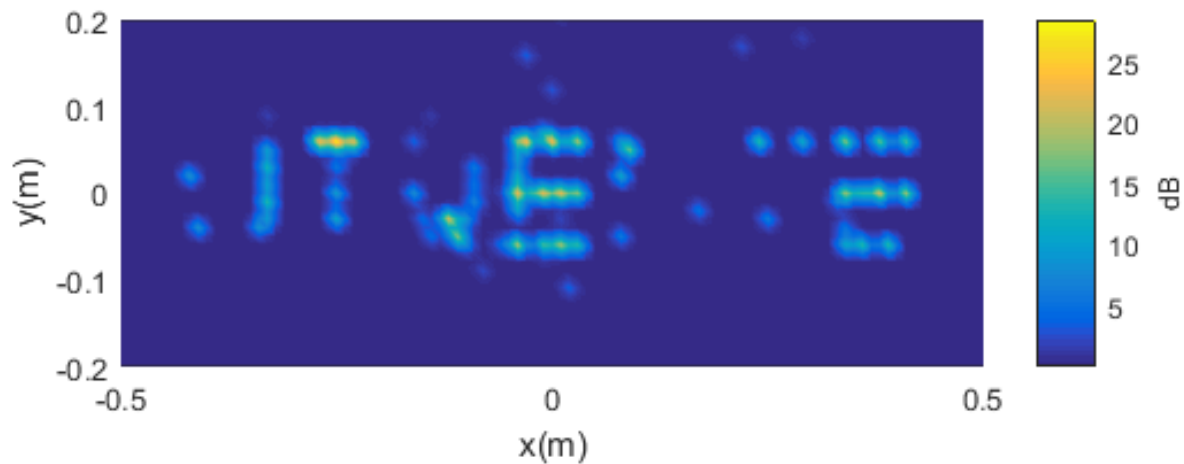
Figure 15: UTwente logo beamformed with CLEAN-SC algorithm now with source of 20 kHz.

[2] Herr, M., "A Noise Reduction Study On Flow-permeable Trailing-edges," Tech. rep., Deutsches Zentrum f?r Luft- und Raumfahrt (DLR), 2007.

[3] Herr, M., "On the Design of Silent Trailing-Edges," *New Results in Numerical and Experimental Fluid Mechanics VI*, Vol. 96, 2008, pp. 430–437.

[4] Sijtsma, P., "Acoustic beamforming for the ranking of aircraft noise," Tech. rep., National Aerospace Laboratory NLR, 2012.

[5] Krober, S., *Comparability of Microphone Array Measurements in Open and Closed Wind Tunnels*, Ph.D. thesis, TU Berlin, 2013.

[6] Oerlemans, S., Sijtsma, P., and Mendez-Lopez, B., "Location and quantification of noise sources on a wind turbine," Tech. Rep. NLR-TP-2007-798, National Aerospace Laboratory NLR, 2007.

[7] Oerlemans, S. and Sijtsma, P., "Acoustic array measurements of a 1:10.6 scaled Airbus A340 model," Tech. rep., National Aerospace Laboratory NLR, 2004.

[8] Arts, T. and for Fluid Dynamics, V. K. I., *Measurement Techniques in Fluid Dynamics: An Introduction*, Von Karman Institute for Fluid Dynamics, 2001.

[9] Mueller, T. J., *Aeroacoustic measurements*, Springer, 2002.

[10] Welch, P. D., "The use of fast Fourier transform for the estimation of power spectra: A method based on time averaging over short, modified periodograms," *Audio and Electroacoustics, IEEE Transactions on*, Vol. 15, No. 2, 1967, pp. 70–73.

[11] Pierce, A. D., *Acoustics: An Introduction to Its Physical Principles and Applications*, Acoustical Society of America, 1989.

[12] Ann P. Dowling, J. E. F. W., *Sound and sources of sound*, Ellis Horwood, 1983.

[13] Rienstra, S. and Hirschberg, A., *An Introduction to Acoustics*, Eindhoven University of Technology, 2012.

[14] Johnson, D. H. and Dudgeon, D. E., *Array Signal Processing: Concepts and Techniques*, Prentice Hall, 1993.

[15] Oerlemans, S., *Detection of aeroacoustic sound sources on aircraft and wind turbines*, Ph.D. thesis, University of Twente, 2009.

[16] Brooks, T. F. and Humphreys, W. M., "A deconvolution approach for the mapping of acoustic sources (DAMAS) determined from phased microphone arrays," *Journal of Sound and Vibration*, Vol. 294, No. 4-5, 2006, pp. 856 – 879.

[17] Underbrink, J. R., *Aeroacoustic Measurements*, chap. Aeroacoustic Phased Array, Springer Verlag, 2002, pp. 98 – 217.

[18] Lallo, M. D., "Experience with the Hubble Space Telescope: 20?years of an archetype," *Optical Engineering*, Vol. 51, No. 1, 2012.

[19] Dougherty, R. P., "Extensions of DAMAS and benifits and limitations of deconvolution in beamforming," 11th *AIAA/CEAS Aeroacoustics Conference*, 2005.

[20] Brooks, T. F. and Humphreys, W. M., "Effect of directional array size on the measurement of airframe noise components," 5th *AIAA/CEAS Aeroacoustics Conference*, No. AIAA-Paper 99-1958, 1999.

[21] Sijtsma, P., "CLEAN Based on Spatial Source Coherence," 13th *AIAA/CEAS Aeroacoustics Conference*, No. AIAA 2007-3436, 2007.